Interactions with titin and myomesin target obscurin and obscurin-like 1 to the M-band – implications for hereditary myopathies

Atsushi Fukuzawa[1,*], Stephan Lange[1,*,‡], Mark Holt[1], Anna Vihola[2], Virginie Carmignac[3,4,§], Ana Ferreiro[3,4], Bjarne Udd[2,5] and Mathias Gautel[1,¶]

[1]King's College London, The Randall Division for Cell and Molecular Biophysics, and Cardiovascular Division, New Hunt's House, London SE1 1UL, UK
[2]The Folkhälsan Institute of Genetics and Department of Medical Genetics, University of Helsinki, Biomedicum, Helsinki, Finland
[3]INSERM, U582, Institut de Myologie, Paris, France
[4]Université Pierre et Marie Curie, Paris, France
[5]Department of Neurology, Vasa Central Hospital, Vasa, Finland

*These authors contributed equally to this work
‡Current address: Department of Medicine, University of California San Diego, USA
§Current address: Department of Experimental Medical Science, Lund University, Sweden
¶Author for correspondence (e-mail: mathias.gautel@kcl.ac.uk)

Accepted 11 March 2008
Journal of Cell Science 121, 1841-1851 Published by The Company of Biologists 2008
doi:10.1242/jcs.028019

Summary

Obscurin, a giant modular muscle protein implicated in G-protein and protein-kinase signalling, can localize to both sarcomeric Z-disks and M-bands. Interaction of obscurin with the Z-disk is mediated by Z-disk titin. Here, we unravel the molecular basis for the unusual localization of obscurin, a Z-disk-associated protein, to the M-band, where its invertebrate analogue UNC-89 is also localized. The first three domains of the N-terminus of obscurin bind to the most C-terminal domain of M-band titin, as well as to the M-band protein myomesin. Both proteins also interact with the N-terminal domains of obscurin-like 1 (Obsl1), a small homologue of obscurin. Downregulation of myomesin by siRNA interference disrupts obscurin–M-band integration in neonatal cardiomyocytes, as does overexpression of the binding sites on either myomesin, obscurin or Obsl1. Furthermore, all titin mutations that have been linked to limb-girdle muscular dystrophy 2J (LGMD2J) or Salih myopathy weaken or abrogate titin-obscurin and titin-Obsl1 binding, and lead to obscurin mislocalization, suggesting that interference with the interaction of these proteins might be of pathogenic relevance for human disease.

Supplementary material available online at
http://jcs.biologists.org/cgi/content/full/121/11/1841/DC1

Key words: M-band, Limb-girdle muscular dystrophy, Myomesin, Obscurin, Titin

Introduction

Assembly of ordered striated myofibrils requires the integration of hundreds of protein subunits in a sequential, regulated way by specific protein-protein interactions. The contractile filaments, composed of actin and myosin subunits, are crosslinked at the Z-disk and M-band, respectively, to give rise to a lateral assembly of molecular machines with nanometre precision. These crosslinks are important to maintain the precise lateral arrangement of actin and myosin during muscle contraction and passive extension (Agarkova and Perriard, 2005). Surprisingly, a number of proteins have recently been localized to both the Z-disk and the M-band, defying concepts of both compartments being biochemically highly specific and mutually exclusive (Lange et al., 2006). The Z-disk and M-band are now recognized as having dual structural and signalling functions, integrating information on mechanical strain with other pathways controlling muscle growth and protein turnover; this integration is achieved by calcium signalling (e.g. via the calcineurin-NFATc pathway at the Z-disk) or by the ubiquitin modification machinery (e.g. via nbr1-p62-MuRF in the M-band) (Lange et al., 2006; Hoshijima, 2006; Linke, 2008). Many of these proteins are targeted to their specific subsarcomeric localization by interactions with the giant modular protein titin [also known as connectin (reviewed in Lange et al., 2006; Tskhovrebova and Trinick, 2003)]. In the M-band, myosin filaments are crosslinked by a protein network composed of titin and proteins of the myomesin gene family, which comprises three *MYOM* genes. *MYOM1* encodes myomesin, which is ubiquitously expressed, *MYOM2* encodes a fast-fibre isoform called M-protein and *MYOM3* encodes myomesin 3, a recently identified isoform of slow fibres (Agarkova et al., 2004; Agarkova et al., 2006; Schoenauer et al., 2008). The M-band-targeting of myomesin relies on the presence of M-band titin, as shown by gene-ablation experiments of this region (Musa et al., 2006). Disruption of the M-band also perturbs sarcomere assembly on a greater scale, affecting the ordered assembly of Z-disks (Musa et al., 2006) and underscoring the importance of coordinated protein interactions for sarcomere integrity.

Obscurin is a recently identified sarcomeric giant protein participating in myofibril organization by forming homotypic interactions between immunoglobulin (Ig)-like domains of the Z-disk portion of titin and Ig-domains near the C-terminus of obscurin (Young et al., 2001). Despite the fact that obscurin was first identified as a binding partner of the titin Z-disk region, the dominant subsarcomeric location of obscurin epitopes in mature myofibrils

Journal of Cell Science

Journal of Cell Science

and cultured cardiomyocytes is the M-band (Bagnato et al., 2003; Borisov et al., 2003; Young et al., 2001); this is also where the nematode analogue of obscurin, UNC-89, is localized (Ferrara et al., 2005). The obscurin gene is differentially spliced in a manner that is complex and, as yet, incompletely understood (Fukuzawa et al., 2005; Russell et al., 2002). The A-isoforms of obscurin contain a C-terminal sequence that binds to the small M-band-localized ankyrin isoforms ankyrin 1.5 and ankyrin 1.9. On the basis of these results, one of the potential roles of obscurin has been suggested to be the tethering of sarcoplasmic reticulum (SR) and contractile apparatus (Armani et al., 2006; Bagnato et al., 2003; Kontrogianni-Konstantopoulos et al., 2003). Although the molecular basis for the differential localization of obscurin to both Z-disks and M-bands is, so far, unclear, the possibility that multiple alternatively spliced variants can be generated from its gene, which is assembled from over 80 exons encoding mostly single domains (Fukuzawa et al., 2005; Russell et al., 2002), might offer an explanation.

Interestingly, the M-band portion of titin at its extreme C-terminus has emerged as a hotspot for autosomal dominant and recessive mutations, causing at least three distinct human myopathies. At present, three different mutations have been reported in *Mex6* (exon 363 of the titin gene), which encodes the last Ig domain (M10). Heterozygous mutations co-segregate with tibial muscular dystrophy patients [TMD; Mendelian Inheritance in Man (MIM)600334], an autosomal dominant late-onset distal myopathy. The more-severe childhood-onset Limb-girdle muscular dystrophy 2J (LGMD2J; MIM608807) phenotype was found to be homozygous for the Finnish TMD founder mutation FINmaj (Udd et al., 2005). The mutations published so far are: (1) a unique 11-bp deletion/insertion at position 293,269-293,279 of the titin gene (FINmaj) that was found to lead to the exchange of four sequential amino acids in M10 in Finnish patients [Glu to Val, Val to Lys, Thr to Glu and Trp to Lys (Hackman et al., 2002)]; (2) a point mutation at position 293,357 that was found to lead to the exchange of Leu to Pro in French patients (Hackman et al., 2002); (3) a point mutation at position 293,329 that was found to lead to the exchange of Ile to Asn in Belgian patients (Van den Bergh et al., 2003). These myopathy-associated mutations of titin M10 suggest the importance of this domain for maintaining functional myofibrils. Recently, an autosomal recessive cardiac and skeletal titin myopathy with two different C-terminal titin deletions encompassing M10 was described (Carmignac et al., 2007), which is also known as Salih congenital muscular dystrophy (Salih et al., 1998; Subahi, 2001).

In this study, we unravel the interactions between the main structural sarcomeric M-band components titin and myomesin with the N-terminal part of obscurin and with a novel protein with similar domain structure to the N-terminal part of obscurin, called obscurin-like 1 (Obsl1). The interaction between titin and obscurin/Obsl1 is decreased or abolished by mutations in titin M10 that are linked to muscular diseases, leading to the disordered association of obscurin/Obsl1 with myofibrils. These results indicate that the incorporation of obscurin/Obsl1 into the sarcomeric M-band is important for myofibril maintenance.

Results

Myomesin interacts with obscurin and obscurin-like 1

Few protein interactions have been unequivocally mapped to myomesin. We therefore carried out yeast two-hybrid (Y2H) screens with several myomesin multidomain constructs in a human cardiac pGAD10 cDNA library. One construct, comprising domains My2 to My6, yielded 40 HIS3- and β-galactosidase-positive clones. Sequence analysis of these prey cDNAs showed that several of them encoded a fragment of a novel protein, predicted by automated computational analysis using the GNOMON gene prediction method and annotated as a predicted cDNA from chromosome 2q35 (NT_005403; GeneID: 23363) in the human genome as Obsl1 (XM_051017). Expressed sequence tags (EST) cDNA entries from human rhabdomyosarcoma GenBank (BC007201), human brain (AB014557) and renal epithelial cells (AK025946) were also found, indicating that Obsl1 expression is not restricted to cross-striated muscle tissues. Analysis of the genomic region on 2q35 using homology searches identified one further N-terminal Ig domain absent from the original GENSCAN prediction. Obsl1 is a modular protein consisting of Ig and fibronectin-like domains, the arrangement of which is identical to that in vertebrate obscurin. A maximum of 20 domains are predicted in Obsl1 compared with 70 in obscurin. In addition to this much smaller size, Obsl1 lacks the SH3-DH-PH domains predicted to act as guanine nucleotide GDP-GTP exchange factors (GEFs), as well as the protein-kinase domains that are a hallmark of obscurin and its invertebrate analogue UNC-89 (Fig. 1).

In agreement with the above observations, we found that Obsl1 expression seems not to be restricted to muscle tissues, but could be detected by northern blot in a variety of human non-muscle tissues as well as smooth muscle (uterus; supplementary material Fig. S1). Weaker expression was found in soleus muscle and cardiac atria, suggesting possible fibre-type-specific expression differences. Reverse transcriptase (RT)-PCR also suggested selective expression of different Obsl1 domains. Domains 4-6 were not detected in several tissues, such as the liver and soleus. RT-PCR revealed robust message levels in the lung, kidney, uterus and cortex, which is in agreement with EST entries (not shown). This suggests that, similar to obscurin, multiple isoforms might be generated by differential splicing, with Ig1 being a constitutive component of the characterized splice isoforms. In agreement with this notion, three EST entries (DA680669, BX381924 and DA427488) were identified in which the first exons, encoding Ig-domains 1-4, are missing (Fig. 1) and the open reading frame starts right after the 5′-untranslated region with Ig5. We therefore raised an antibody against the Ig1 domain of Obsl1 in rabbit to locate the protein in sarcomeres. We found that, in neonatal rat cardiomyocytes (NRCs), anti-Obsl1-Ig1 stained the M-band and thus co-localized with M-band titin and myomesin, as well as with obscurin. In skeletal muscle, we also found M-band staining that was predominantly myofibrillar (supplementary material Fig. S2D). This lends excellent support to the interaction data that led to the identification of Obsl1.

Several overlapping fragments were generated to map the interaction between myomesin and Obsl1 more precisely. Obsl1 constructs containing domain Ig3 were able to bind myomesin both in Y2H and pulldown assays (Fig. 2A,B). Similarly, the binding site for Obsl1 on myomesin was mapped to the linker region between domains My4 and My5 (Fig. 2A). Because of the homology of sequence and domain pattern between Obsl1 and obscurin, we tested whether also domain 3 of obscurin (Ob-Ig3) could bind the same region in myomesin. Ob-Ig3 interacted in the same way as Obsl1, suggesting that the homology of both proteins also reflects functional homology of their interaction capacity (Fig. 2A,B).

The human genome contains three myomesin-like genes, *MYOM1*, *MYOM2* and *MYOM3*. The obscurin-binding linker between domains My4 and My5 is, however, only weakly conserved between these three homologues (Fig. 2C), with M-protein showing the highest similarity to myomesin. We therefore tested whether

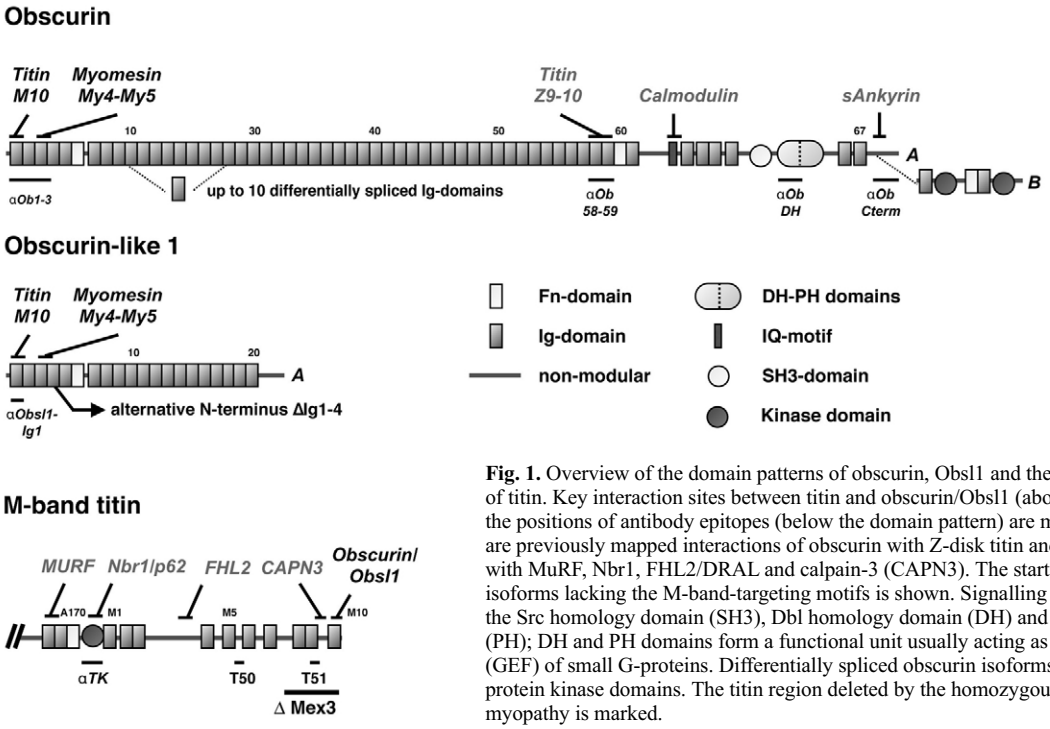

Fig. 1. Overview of the domain patterns of obscurin, Obsl1 and the C-terminal M-band-portion of titin. Key interaction sites between titin and obscurin/Obsl1 (above the domain pattern) and the positions of antibody epitopes (below the domain pattern) are marked. Also shown (in grey) are previously mapped interactions of obscurin with Z-disk titin and ankyrin, and M-band titin with MuRF, Nbr1, FHL2/DRAL and calpain-3 (CAPN3). The start of the alternative obscurin isoforms lacking the M-band-targeting motifs is shown. Signalling domains in obscurin include the Src homology domain (SH3), Dbl homology domain (DH) and pleckstrin homology domain (PH); DH and PH domains form a functional unit usually acting as a GDP-GTP exchange factor (GEF) of small G-proteins. Differentially spliced obscurin isoforms can also contain up to two protein kinase domains. The titin region deleted by the homozygous *Mex3* mutation in Salih myopathy is marked.

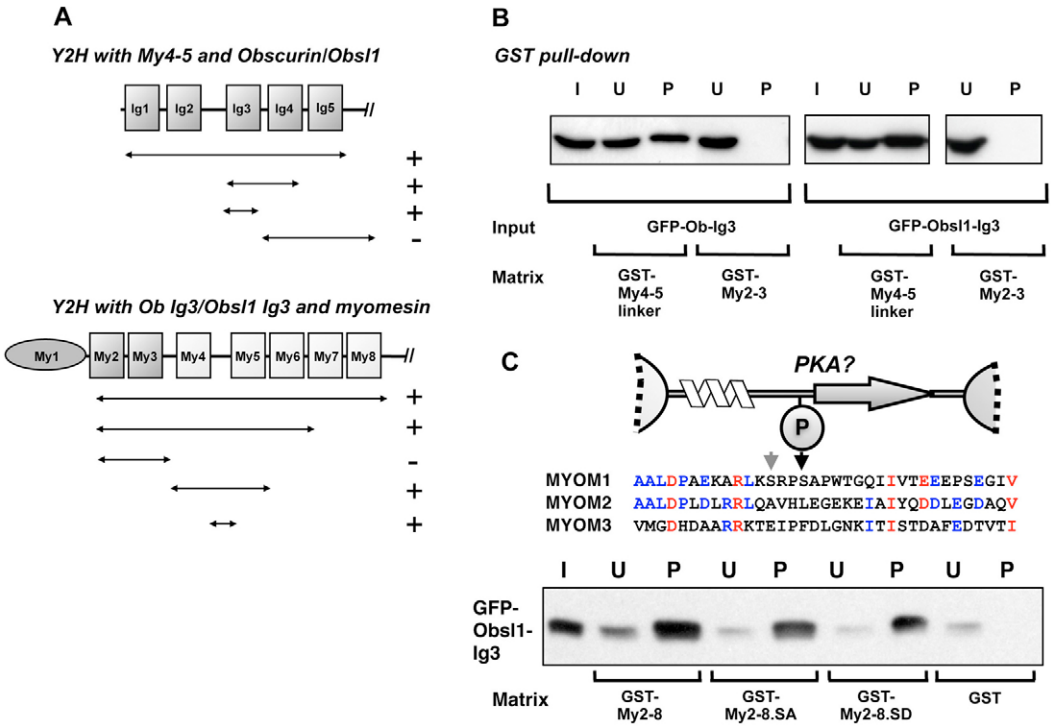

Fig. 2. Interaction of the N-terminal region of obscurin/Obsl1 with myomesin. (A) Sub-mapping of the minimal binding domain of obscurin/Obsl1 to My4-My5 and of myomesin to obscurin/Obsl1 Ig3 by successive deletion mutants of My2-My8 using Y2H assays identified Ig3 of obscurin/Obsl1 (top) and the linker between My4 and My5 of myomesin (bottom) as sufficient for binding. (B) These interactions were verified by pulldown assays using GST–My4-My5-linker bound to glutathione beads and GFP-tagged obscurin/Obsl1 Ig3 constructs. (B,C) Detection was performed by blotting equivalent amounts of input (I), unbound (U) and bound (P) fractions with anti-GFP antibody. (C) The interaction of obscurin/Obsl1 Ig3 with the linker between myomesin My4 and My5 is specific for myomesin and is not regulated by phosphorylation. (C, top) Predicted secondary structure of the My4-My5 linker with the protein kinase A (PKA) site. (C, middle) Alignment of the linker sequence of the three myomesin gene family members, *MYOM1-MYOM3*, with the phosphorylated serine is shown by a black arrow, the neighbouring serine 615 is shown by the grey arrow; red, residues conserved in all three genes; blue, residues conserved only in two *MYOM* genes. (C, bottom) Pulldown assay with mutation of the phosphorylated serine 618 in *MYOM1* to alanine (SA) or aspartate (SD).

Journal of Cell Science

M-protein could also bind obscurin and Obsl1, and found that this interaction was observed only for the ubiquitously expressed myomesin (not shown). The obscurin/Obsl1-binding linker in myomesin contains a potential phosphorylation site for PKA-like kinases that was reported to modulate an interaction with titin M4 in dot-blot assays (Obermann et al., 1997). To test whether this site might be involved in regulating the myomesin-obscurin interaction, we generated point mutations in the motif KARLKSRPS*, exchanging the phosphorylated serine 618 for aspartate (SD, phospho-mimicry mutant) or alanine (SA, non-phosphorylatable). Both mutants showed unaltered ability to bind Obsl1 (Fig. 2C) and obscurin (data not shown), suggesting that the interaction of myomesin with obscurin/Obsl1 is not regulated by myomesin phosphorylation. Similarly, mutation of the neighbouring serine 615 showed no influence on obscurin/Obsl1 binding (data not shown). However, neither in Y2H assays nor in pulldown assays could we reproduce the previously reported interaction of the My4-My5 linker region (abbreviated to My4-My5) with titin M4 (not shown).

Titin M10 interacts with the N-terminus of obscurin and Obsl1 – titin, obscurin and myomesin can form a ternary complex

To corroborate the interaction results in a parallel approach, we searched for ligands of the N-terminal region of obscurin or Obsl1 in Y2H screens. Using Ig-domains 1-5 of obscurin as bait, five HIS3- and β-galactosidase-positive clones were identified from a human cardiac cDNA library and were analyzed by sequencing. Two of these contained identical inserts derived from the N-terminal part of myomesin, comprising the linker region between My4 and My5. This result is in excellent agreement with the interaction we identified independently for obscurin and Obsl1 using the myomesin bait.

The remaining three clones all encoded the most C-terminal part of titin. The smallest clone delimited the minimum binding site on titin to the insertion Is7 and the C-terminal Ig-domain M10 of titin. In order to further narrow down the minimum binding sites on both titin and obscurin, a series of truncation constructs were analyzed for binding in forced Y2H assays. As shown in Fig. 3A, only constructs containing titin M10, but not those containing only Is7, showed binding to obscurin, whereas obscurin Ob-Ig1 was sufficient for titin M10 binding. The binding between titin M10 and obscurin Ig1 was confirmed by GST pulldown assays (Fig. 3B).

Because of the functional homology of obscurin and Obsl1 with respect to myomesin binding, we investigated whether Ig1 in Obsl1 was also able to bind to the C-terminal Ig-domain M10 in titin. Y2H and pulldown assays demonstrated comparable interaction between Obsl1-Ig1 and titin M10 (Fig. 3A,B). This result substantiates a strong functional homology for the N-terminal part of obscurin and Obsl1.

The arrangement of titin- and myomesin-binding sites on successive, individual domains on obscurin suggests that they might function independently. To test this hypothesis, we analyzed the ability of obscurin fragments to bind to titin and myomesin simultaneously. Myomesin My4-My5 did not show appreciable binding to titin M10 (Fig. 3C). In the presence of My4-My5, obscurin Ig1-Ig2 bound to titin M10, with no binding of the myomesin fragment. However, when this experiment was carried out with obscurin Ig1-Ig3, a fragment encompassing both the titin- and myomesin-binding sites, both obscurin and myomesin My4-

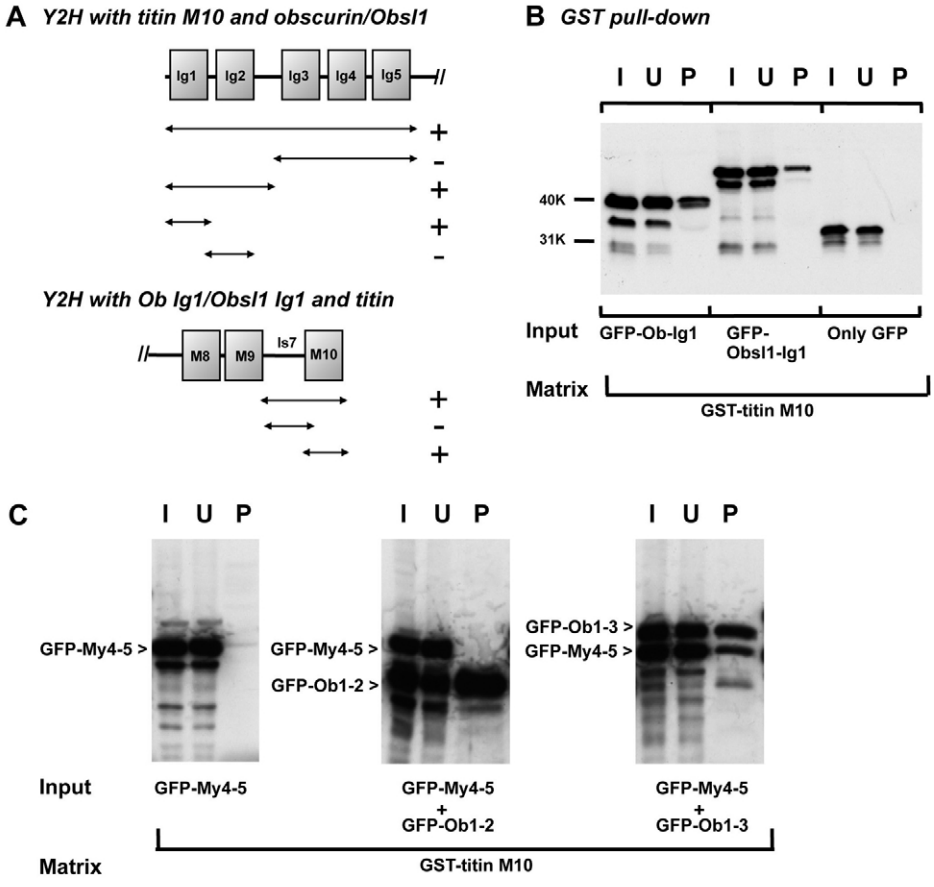

Fig. 3. Interaction of the N-terminal region of obscurin/Obsl1 with titin. (A) Sub-mapping of the minimal binding domain of obscurin/Obsl1 to titin M10 and of titin to obscurin/Obsl1 Ig1 by Y2H assays identified that Ig1 of obscurin/Obsl1 (top) and M10 of titin (bottom) are sufficient for the binding. (B) These interactions were also verified by pulldown assays using GST-M10 bound to glutathione beads and GFP-tagged obscurin/Obsl1 Ig1 constructs. Detection was performed by blotting equivalent amounts of input (I), unbound (U) and bound (P) fractions with anti-GFP antibody. (C) Ternary-complex formation between obscurin, titin and myomesin in pulldown assays. GST–titin-M10 beads were incubated with GFP–My4-My5 alone (left) and in the presence of obscurin Ob-Ig1-Ig2 (middle) or Ob-Ig1-Ig3 (right). Ob-Ig1-Ig2 binds to titin M10, but myomesin My4-My5 is only bound when the binding site on Ob3 is present, demonstrating the formation of a ternary complex by independent binding motifs.

My5 were found in the titin-bound fraction, demonstrating that obscurin can target myomesin to titin M10 (Fig. 3C). These results also demonstrate that the interaction of titin and myomesin with obscurin are mutually independent, and that the obscurin and Obsl1 N-termini can function as a crosslinker between titin and myomesin.

Overexpression of the minimal binding sites in obscurin, myomesin or titin disrupts endogenous obscurin localization

Would disruption of either the titin or myomesin interaction therefore lead to altered sarcomeric localization of obscurin? We addressed this important question in NRCs that were transfected with Ob-Ig1 (the binding site for titin), or Ob-Ig3 (the binding site for myomesin) fused to GFP. In Ob-Ig1-transfected cells (Fig. 4), the staining of anti-obscurin antibodies (here anti-Ob58-59) at the M-band was weakened compared with non-transfected cells (Fig. 4) or Ob-Ig2-transfected cells (not shown). Quantitative image analysis showed that the apparent ratio of obscurin to titin was reduced from about 2:1 down to 1:1. In contrast to endogenous obscurin, the intensity and location of the T51 antibody epitope in the M9 Ig domain of titin (Obermann et al., 1996) close to M10 was not changed by exogenous Ob-Ig1 overexpression (Fig. 4). Similarly, this dominant-negative effect on endogenous obscurin was also observed for Obsl1-Ig1- and titin-M10-transfected cells (Fig. 4).

The effect of exogenous fragments on endogenous obscurin was even more striking in cells that had been transfected with Ob-Ig3 or the My4-5 linker region. Transfection of both constructs weakened the signal of anti-obscurin antibodies at the M band, displaying a completely diffuse localization of endogenous obscurin in the cytoplasm (Fig. 5A, top and bottom rows). The effect of Ob-Ig3 on the correct localization of obscurin could be reproduced with the homologous Ig3 in Obsl1 (Fig. 5A, middle row), again indicating a functional homology between these two proteins. In about one tenth of Obsl1-Ig3-transfected cells, sarcomere structure was additionally disrupted and obscurin formed broad doublet stripes (Fig. 5A and insert). In contrast to the linker region in myomesin, the homologous linker region in M-protein showed no effect on obscurin localization (data not shown). This result corroborates our previous pulldown data and confirms that only myomesin, but not M-protein, is able to bind to obscurin or Obsl1.

The effect of exogenous Obscurin/Obsl1 Ig3 or My4-My5 domains on endogenous Obsl1 was similar to that on endogenous obscurin, with the loss of defined M-band striation and a diffuse pattern (Fig. 5B). As with obscurin (Fig. 4, bottom row), transfection of titin M10 had the most subtle effect (not shown), and My4-My5 the most severe dominant-negative effect (Fig. 5B). Due to the specificity of our antibody against Obsl-Ig1, the effect of exogenous Obsl1-Ig1 on endogenous Obsl1 could not be tested. When we transfected the dominant-negative constructs into C2C12 myoblasts, we could not observe surviving GFP-positive cells with discernable sarcomeres (not shown), suggesting also a strong dominant-negative effect on de novo sarcomere formation.

The dominant-negative effects of transfected obscurin fragments in cultured cardiomyocytes firmly support the concept that obscurin is incorporated into the M-band via the interactions of Ob-Ig1 and Ob-Ig3 with titin and myomesin.

Intriguingly, no changes in the correct localization of either titin or myomesin at the microscopic level were observed after transfection of any constructs that affect the correct localization of obscurin to the sarcomeric M-band. This suggests that obscurin localization depends on both myomesin and M-band titin, but not vice versa.

siRNA-mediated knockdown of myomesin results in an aberrant localization of obscurin and unordered sarcomeres

Because myomesin seemed to be a major determinant for the correct integration of obscurin into the sarcomere, we investigated whether

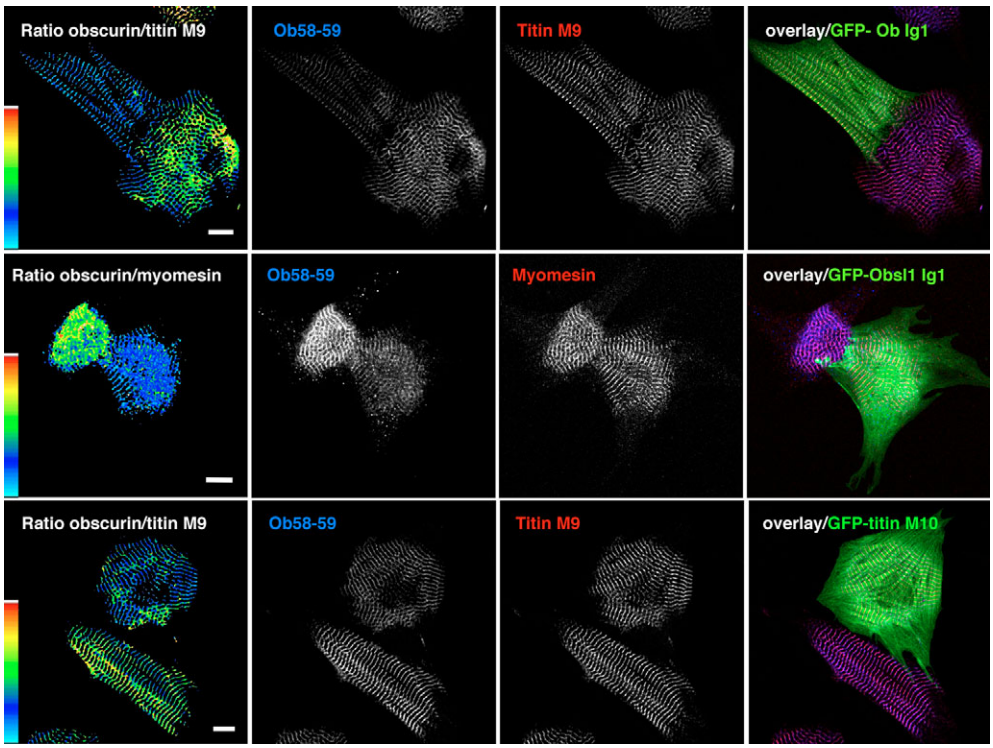

Fig. 4. Localization of endogenous obscurin in NRCs transfected with components of the obscurin-Obsl1-titin complex. Overexpression of the titin-binding site in obscurin or Obsl1 (Ob-Ig1 or Obsl1-Ig1, respectively) leads to loss of endogenous obscurin (Ob58-59) from the M-band. Similarly, transfection of titin M10 reduces M-band-bound obscurin. Titin-normalized obscurin channel analysis of obscurin and/or titin, individual channels and overlay are shown. Range indicator indicates a range of 0 (black) to 3 (white). Scale bars: 10 μm.

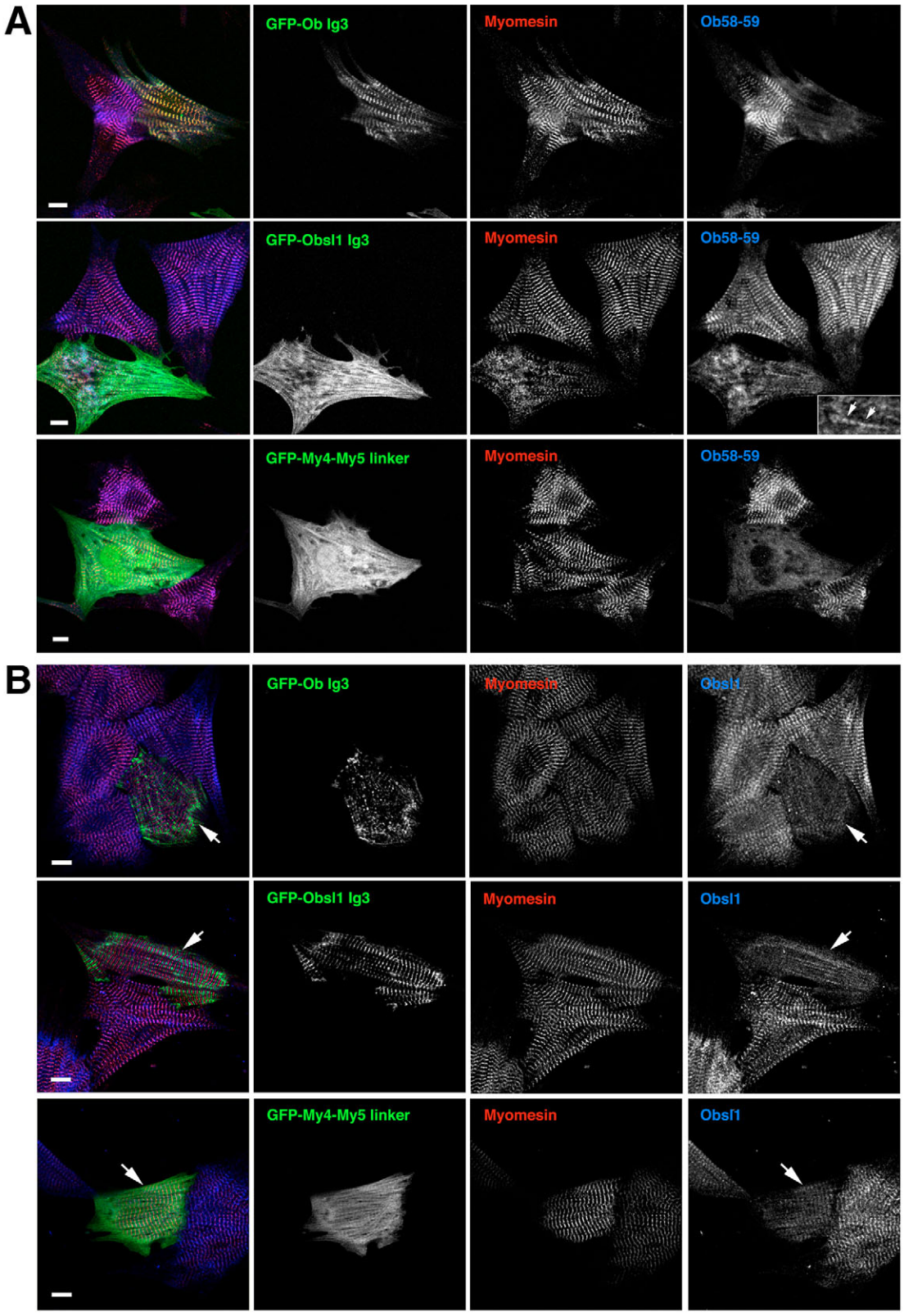

Fig. 5. Endogenous obscurin localization in NRCs transfected with fragments related to obscurin/Obsl1-myomesin interaction. (A) Overexpression of the myomesin-binding third Ig domains of obscurin (Ob-Ig3) or Obsl1 (Obsl1-Ig3) leads to loss of endogenous obscurin (Ob58-59) from the M-band. Note the strong reduction of obscurin M-band staining with diffuse localization in the transfected cells, visualized by GFP fluorescence of the tagged transfected constructs. Similarly, transfection of the myomesin My4-My5 linker leads to a reduction of M-band-bound obscurin with broad, fuzzy stripes. Overlay and individual channels are shown. (Inset) Twofold-magnified area of the same image showing broad doublet stripes (arrows). (B) Endogenous Obsl1 in NRCs transfected with fragments related to obscurin/Obsl1-myomesin interaction. Overexpression of the myomesin-binding third Ig domains of obscurin (Ob-Ig3) or Obsl1 (Obsl1-Ig3) leads to loss of endogenous Obsl1 from the M-band. Note the reduction of Obsl1 M-band staining with diffuse localization in the transfected cells, visualized by GFP fluorescence of the tagged transfected constructs. Similarly, transfection of the myomesin My4-My5 linker leads to a reduction of M-band-bound Obsl1, with broader, fuzzy stripes (arrows). Scale bars: 10 μm.

the reduction of endogenous myomesin would also affect obscurin localization, comparable to the overexpression of the minimal binding sites. By transfecting a myomesin siRNA vector into NRCs, we achieved strong perturbation of the endogenous myomesin pattern (Fig. 6). The remaining myomesin largely failed to assemble into ordered M-band stripes, probably because disruption of the structural links between myomesin and myosin, titin or obscurin leads to a general failure in the coordinated assembly of the M-

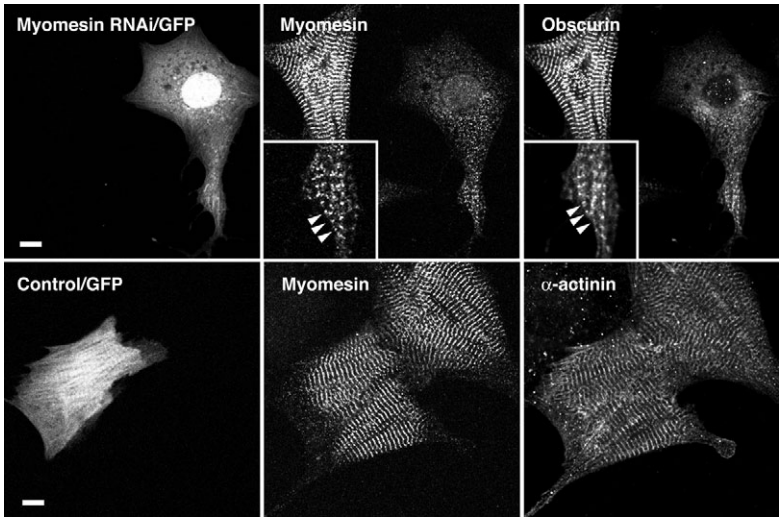

Fig. 6. Downregulation of myomesin by siRNA interference disrupts M-band structure and leads to loss of obscurin striations in NRCs. NRCs transfected with myomesin siRNA, visualized by GFP fluorescence, show dramatically reduced myomesin levels with loss of M-band striations. Obscurin is diffusely localized in cells treated with siRNA, except for in areas of residual myofibrils, in which it colocalizes with myomesin (arrowheads in insets). Control cells transfected with unspecific siRNA vector show no change in the localization of obscurin or sarcomeric markers (α-actinin). (Inset) Twofold-magnified area of the same image showing residual primitive stripes. Scale bars: 10 μm.

band. The localization of obscurin in siRNA-transfected cells was also generally cytoplasmic and lacked an ordered sarcomeric striation pattern (Fig. 6). Occasional weak association with myomesin in rudimentary stripes could be observed (Fig. 6, inset). Considering the results of overexpression experiments, it appears, therefore, that both titin and myomesin interactions are required to target obscurin, and probably Obsl1, to the M-band.

Myopathy mutations in titin M10 abolish its ability to bind obscurin, and disrupt M-band-bound obscurin

Because obscurin and Obsl1 are presently the only known sarcomeric interaction partners for the C-terminal Ig-domain M10 of titin, we were interested to see whether the disease-associated mutations in titin M10 affect its binding to obscurin.

To clarify this issue, a forced Y2H assay was performed that compared the binding of obscurin to the Ig-domain M10 of titin, with all published titin *Mex6* (exon 363) mutations from human muscular dystrophy patients being mimicked (Fig. 7A). As expected, wild-type M10 showed growth on selective media and β-galactosidase activation. By contrast, M10 containing the Finnish or French TMD mutations did not show either reporter gene activation, indicating absent or strongly weakened interaction. Unlike the Finnish and French mutations, the Belgian TMD mutation showed positive reporter gene activities, similar to wild type. The effects of TMD and/or LGDM2J mutations on obscurin binding were confirmed by a GST pulldown assay (Fig. 7B). In agreement with the forced Y2H results, Ob-Ig1 showed robust binding to both wild-type M10 and the Belgian TMD mutation, but not to the Finnish or French mutant M10. Despite completely negative Y2H responses for the French and Finnish mutations, very weak binding of Obsl1-Ig1 to these mutant forms of M10 could be observed. Attempts to quantify the interaction strength of the mutant domains by biosensor assays were thwarted by very low-affinity, non-saturable binding. Whether this apparent residual, very weak interaction is functionally sufficient to maintain the M-band functions of Obsl1 will require further structural and biophysical analysis.

Both results strongly indicate that the mutations found in the TMD and LGMD2J patients decrease or abolish the binding ability of titin to obscurin, and the loss of interaction between titin and obscurin might be an important feature of these diseases.

We therefore wanted to investigate the location of obscurin and Obsl1 in biopsies of LGMD2J (titin *Mex6*, exon 363, Finnish homozygous) as well as Salih myopathy (titin *Mex3* deletion, exon 360) patients. It was previously confirmed in muscle biopsies from these myopathies that the M8-M9 titin epitope was lost completely, whereas the nearby A169-A170 titin epitopes were normally localized to the M-band, as was myomesin (Carmignac et al., 2007; Hackman et al., 2002). We therefore stained the limited available cryosections of affected, as well as control, muscles for obscurin and myomesin. In the affected muscles, obscurin lost its sharply defined M-band localization in LGMD2J *Mex6*-mutant M-bands and was severely mislocalized in Salih myopathy *Mex3*-mutant M-bands. This was observed even in areas in which M-band structure labelled by anti-myomesin antibodies appeared normal; obscurin also did not relocalize to the binding site at the Z-disk (Fig. 7C).

Discussion

Here, we report the ternary interaction between the M-band-associated C-terminal portion of titin, the N-terminus of obscurin and an interdomain linker in the M-band protein myomesin; this interaction is responsible for targeting obscurin and its small homologue Obsl1 to the M-band. We have shown previously that obscurin locates mainly at the M-band in mature striated muscle (Young et al., 2001). Considering these observations, the interactions of obscurin with both myomesin and the C-terminal M10 domain of titin identified here are likely to be biologically meaningful. These interactions explain a number of previously unclear observations, ranging from the subcellular localization of obscurin to previously unknown interaction partners for the C-terminus of titin. Our findings also provide a rationale for understanding the pathomechanism of the M-band titin-linked hereditary myopathies Salih myopathy (Carmignac et al., 2007) and LGMD2J (Udd et al., 2005).

Obscurin and obscurin-like 1

The giant modular protein obscurin was first identified in Y2H screens with Z-disk portions of titin (Young et al., 2001). Surprisingly, however, adult muscles show obscurin at the sarcomeric M-band with only occasional weaker Z-disk staining. This suggests a second sarcomeric binding site responsible for M-band targeting. The interactions of the obscurin N-terminus with titin M10 and

Journal of Cell Science

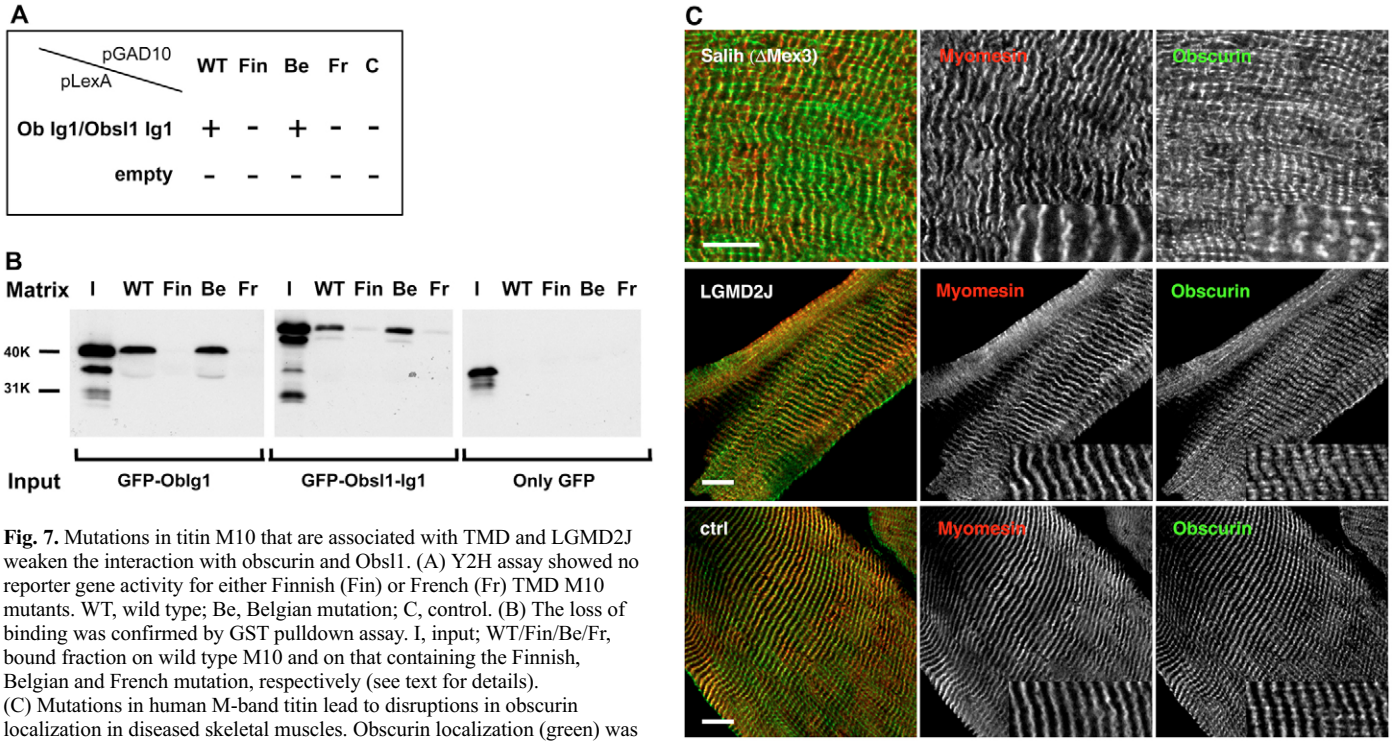

Fig. 7. Mutations in titin M10 that are associated with TMD and LGMD2J weaken the interaction with obscurin and Obsl1. (A) Y2H assay showed no reporter gene activity for either Finnish (Fin) or French (Fr) TMD M10 mutants. WT, wild type; Be, Belgian mutation; C, control. (B) The loss of binding was confirmed by GST pulldown assay. I, input; WT/Fin/Be/Fr, bound fraction on wild type M10 and on that containing the Finnish, Belgian and French mutation, respectively (see text for details). (C) Mutations in human M-band titin lead to disruptions in obscurin localization in diseased skeletal muscles. Obscurin localization (green) was compared with that of myomesin (red) in confocal analysis of cryosections of patient biopsies. In the presence of the Salih myopathy homozygous *Mex3* deletion, general M-band morphology is disrupted, as shown by irregular myomesin striations. Even in areas with relatively normal-appearing myomesin stripes, obscurin is disrupted and localizes to split bands and longitudinal streaks, and diffusely. In skeletal muscles from LGMD2J patients, myomesin striations appear relatively normal, in agreement with the less-severe nature of the titin mutation. Obscurin is found in broad and diffuse stripes over the M-band, with loss of the tight colocalization with myomesin seen in normal control (ctrl) muscles. (Insets) Magnified 2×. Scale bars: 10 μm.

myomesin, two well-characterized M-band components, now establish this 'missing link'. It furthermore lends strong support for a transverse orientation of obscurin with respect to the sarcomeric filament axis, with the N-terminus being myofibril-bound and the ankyrin-binding C-terminus most probably being associated with the SR enveloping the sarcomere. We also identified a new interaction of myomesin and titin with Obsl1, a smaller modular protein with patterns of Ig and fibronectin (Fn)3-like domains highly similar to the N-terminal part of obscurin. Homologous domains in Obsl1 interacted with titin and myomesin. Obsl1 lacks the ankyrin-binding non-modular region found in obscurin-A and also, unlike obscurin-A and obscurin-B, contains no signalling domains. The major function of this new protein might therefore be structural, possibly adding an additional layer of crosslinks between myosin filaments. During the preparation of this manuscript, Obsl1 was described as a protein of the M-band, Z-disk, intercalated disk, nuclear lamina and cytosol (Geisler et al., 2007). The antibodies purified for this study, however, show marked M-band localization, which is only disrupted by the dominant-negative effects of myomesin, titin or the binding domains to these on Obsl1 itself (supplementary material Fig. S2). We also found that the N-terminus of Obsl1 contains five instead of four Ig domains, which would be in agreement with the highly homologous domain structure in the N-terminus of obscurin (Fig. 1). Furthermore, we identified novel splice variants of Obsl1 that lack the N-terminal domains responsible for titin and myomesin interaction. It is possible, therefore, that the puzzlingly complex picture of Obsl1 localization observed by Geisler et al. (Geisler et al., 2007) relates to those isoforms lacking the M-band-targeting domains 1-3.

Previous siRNA knockdown experiments of obscurin suggested that obscurin might be necessary for the lateral alignment of myofibrils and for sarcomere assembly (Kontrogianni-Konstantopoulos et al., 2006). However, the total loss of M-band-bound obscurin upon transfection of My4-My5, with completely preserved myofibril structure and lateral alignment even after prolonged culture of these cardiomyocytes (Fig. 5A), suggests that the phenotype of a total knockdown of obscurin is not explained by crosslinking myofibrils at the M-band. Rather, because siRNA knockdown will abolish the entire molecule, including the SR-linking C-terminus and the C-terminal GEF and kinase domains, it seems possible that the knockdown of obscurin signalling functions and/or SR anchorage might be responsible for the observed siRNA phenotypes. Intriguingly, competing obscurin out of the M-band does not lead to its association with the Z-disk, suggesting that Z-disk and M-band sorting might not be competitive processes but regulated on another level, possibly by alternative splicing or posttranslational modifications.

Myomesin

Our analyses show that myomesin plays a far more complex role in M-band formation than previously expected. Apart from being a crosslinker of myosin filaments and an anchor of titin, it is also crucially involved in targeting obscurin and Obsl1 to the M-band. Our siRNA knockdown experiments furthermore suggest that the presence of M-band titin and obscurin alone is insufficient for M-band formation in the absence of myomesin, leading to total destruction of not only the M-band but of overall myofibril structure. This phenotype is reminiscent of the homozygous ablation

Journal of Cell Science

Journal of Cell Science

of M-band titin in embryonic stem (ES)-cell derived cardiomyocytes (Musa et al., 2006), underscoring the importance of the interdependent network of M-band proteins for structural stability.

The human and mouse genomes contain three myomesin genes (*MYOM1*, *MYOM2* and *MYOM3*). Only the product of *MYOM1*, myomesin, was able to bind to obscurin/Obsl1. The expression of myomesin (*MYOM1*) and M-protein (*MYOM2*) is fibre-type specific, with M-protein being expressed predominantly in fast fibres of the mouse (Agarkova et al., 2003). Varying stoichiometry of titin and myosin to the MYOM family members could thus lead to fibre-type-specific differences in the stability of the ternary complex of titin, myomesin proteins and obscurin/Obsl1.

Titin

Our data show for the first time in detail how the extreme C-terminus of titin is involved in protein-protein interactions with structural M-band proteins. The ternary complex between the first three Ig domains of obscurin, the interdomain linker between My4 and My5 of myomesin, and titin M10 places all three proteins in a spatially strictly confined context that is limited by the 4-nm dimensions of the Ig domains. Previously, dot-blot analysis had indicated an interaction between titin M4 and myomesin domains My4 and My6, which might be regulated by myomesin phosphorylation (Obermann et al., 1997). We therefore verified this interaction by two independent methods, Y2H analysis and pulldown assays. In both assays, we could not confirm the titin-M4–myomesin interaction. Furthermore, contrary to the transfection of titin M10, Ob-Ig1 or Ob-Ig3 and the homologous domains in Obsl1, transfection of titin M4 had no effect on M-band localization of myomesin (data not shown). We conclude that this interaction is unlikely to be physiologically significant for static M-band structure but cannot rule out that it might be transiently involved during M-band assembly. Interestingly, the interaction of myomesin and obscurin Ig3 in the same region is not dependent on phosphorylation, suggesting that it is static rather than dynamic. Together with previous ultrastructural and interaction data, our data therefore provide new spatial constraints for modelling the M-band (Fig. 8). Titin and myomesin domains have previously been localized by immuno-electron microscopy (Obermann et al., 1996). Because the size of the primary and secondary antibody complexes used as label in this study is large (ca 30 nm) compared with the size of the M-band, and epitope access in the tight myofibril lattice is spatially limited, leading to possible errors in defining the epitope as the centre of mass, these domain positions may be considered as guidelines rather than absolute measures. We have therefore based our revised M-band model on the positional constraints posed by the protein interactions defined here and on the general orientation of titin and myomesin revealed by electron microscopy.

Recently, two genetic models with specific homozygous ablation of the M-band region were shown to disrupt sarcomere assembly or stability. An internal deletion of M-band titin, including domains A169 to M7, leads to progressive sarcomere failure and muscle atrophy in skeletal muscle, and, when activated in cardiac muscle, to hypertrophic failure, most probably of a secondary nature (Gotthardt et al., 2002; Peng et al., 2006; Peng et al., 2007). Interestingly, cardiac sarcomeres in the constitutive-deletion model of A169 to M7 formed initially, but then failed under increasing haemodynamic stress.

In contrast to this partial failure of sarcomere maintenance, the total homozygous ablation of M-band titin, including M8 to M10, leads to a complete disruption of primary myofibrillogenesis in

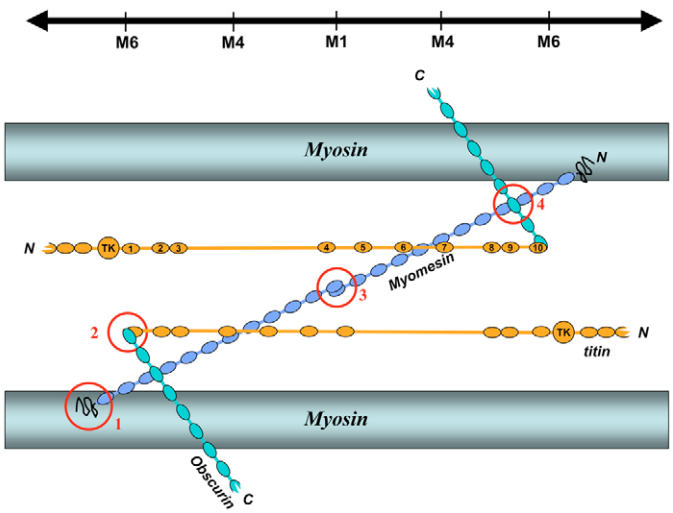

Fig. 8. Model of the M-band incorporating the spatial constraints on the localization of titin, myomesin and obscurin on the basis of the protein interactions identified here and previously. The M-band lines are marked at the top of the figure. The path of titin is unknown outside the M-band, hence no precise arrangement is shown from the domains immediately N-terminal to the kinase domain. Ig and Fn3 domains are shown as ovals, the titin kinase domain (TK) as a circle and the interdomain-sequence insertions as lines. Titin M-band domains are numbered. Protein interactions are: (1) myomesin My1 and myosin; (2) obscurin/Obsl1 Ig1 with titin M10; (3) myomesin homodimerization via My13; and (4) obscurin/Obsl1 Ig3 with myomesin My4-My5. Note that this model makes no assumptions on whether titin crosses over between myosin filaments or is arranged in a strictly parallel fashion, but mechanical considerations make a crosslinking titin arrangement more plausible.

targeted ES-cell-derived cardiomyocytes (Musa et al., 2006), with diffuse localization of obscurin and myomesin. Comparison of the two phenotypes suggests that crucial interactions allowing minimal M-band formation must reside in titin domains M8 to M10. The interactions of M10 with obscurin and Obsl1 seem to contribute to M-band stability, although M-bands are at least temporarily stable when obscurin is completely diffuse (see Fig. 5A). The different phenotypes of the two genetic titin-M-band-deletion models could thus be explained by residual M10 interactions in the internal deletion model, linking the remaining M-band titin fragment to myomesin via obscurin/Obsl1.

Implications for hereditary myopathies

A number of human titin M-band mutations have recently been identified that cause autosomal recessive or dominant myopathies. Among them, tibial muscular dystrophy and LGMD2J are caused by mutations in the titin domain M10 (Udd et al., 2005). Clinical severity correlates to the expected biochemical effects of the mutations. The Finnish and French mutations disrupt key structural features of the M10 Ig-fold and are clinically characterized as more severe compared with the Belgian TMD mutation, which is a structurally less-severe missense mutation in the β-barrel. The clinically more-severe mutations reduce titin-obscurin/Obsl1 binding severely, whereas binding by the Belgian TMD mutation is not detectably reduced [although small differences in the diffusion coefficient (K_d) would escape our assays and might still be pathomechanistically significant]. Interestingly, the biochemical findings are reflected by the absence of M-band-localized/mislocalized obscurin in LGMD2J homozygous muscle samples despite preserved M-band structure and normal lateral

Journal of Cell Science

alignment of myofibrils. These observations suggest that loss of M-band obscurin has no immediate consequences on sarcomere stability and myofibril order, or on their lateral alignment in humans. Defects in the precise spatial arrangement of excitation-contraction coupling could also explain the phenotype of the aforementioned siRNA and morpholino experiments (Raeker et al., 2006).

A new group of severe, autosomal recessive titinopathies was recently identified, in which premature stop codons in titin exons *Mex1* and *Mex3* (exons 358 and 360) cause deletions of the C-terminal part of M-band titin, encompassing domains M5 to M10 and M8 to M10, respectively (Carmignac et al., 2007). Although the affected region in these mutations encompasses further binding sites, such as that for calpain-3, the presence of a cardiac phenotype suggests that loss of obscurin/Obsl1 is likely to be involved (because calpain-3 is not expressed in heart muscle).

In summary, we have identified the M-band-targeting mechanism for the giant multicompartment protein obscurin and its smaller homologue Obsl1. These findings are of relevance for several hereditary human myopathies involving loss of this binding site on titin. In addition, these observations provide crucial insight into the molecular interactions relevant for M-band assembly and provide physical constraints relevant for structural models of the M-band.

Materials and Methods

Yeast two-hybrid screening

Y2H screening was essentially performed as described previously (Young, 1998). pLex-My2-6 or Ob-Ig1-5 were co-transformed with pGAD10 human cardiac muscle cDNA library into NMY51 yeast strain by standard procedure. Transformants were screened by *HIS3* reporter gene activity, and then selected clones were re-selected by *Ade2* reporter gene activity and *lacZ* activity.

RNAi constructs

The RNAi vector H1-GFP-cDNA3.1-Zeo was derived from inserting the coding sequence of EGFP (Clontech) into pcDNA3.1-Zeo (Invitrogen), enabling detection for transfected cells by fluorescence, and insertion of the H1-promotor RNAi cassette of the pSuper vector [(Brummelkamp et al., 2002), kind gift of R. Agami, The Netherlands Cancer Institute, Amsterdam, The Netherlands] into GFP-pcDNA3.1-Zeo. RNAi constructs for myomesin were generated by linker ligation into H1-GFP-cDNA3.1-Zeo using the following oligos: Myom, 5′-GATCCCCtatggctcggagaccagcgTTCAAGAGAcgctggtctccgagccataTTTTTGGAAA-3′ and Myom, 3′-AGCTTTTCCAAAAAtatggctcggagaccagcgTCTCTTGAAcgctggtctccgagccataGGG-5′ (lowercase nucleotides indicate the homologous complementary sequences of the hairpin). The sequence and correct integration was verified by sequencing. Co-transfections of the siRNA construct with HA-labelled myomesin and M-protein constructs in COS cells confirmed the specificity to myomesin.

Mutagenesis

Site-directed mutagenesis was carried out using a modified version of the QuikChange protocol (Stratagene). All nucleotide numbers corresponded to NM003319/GenBank [*Homo sapiens* titin (TTN), transcript variant N2-B]. Mutated nucleotides are shown in capitals. (1) Finnish mutation primer: 5′-gggtgagcctaccccagTGAAAGAAAAAtcctgtggtggaagaaaaatcc-3′, 80791-80840. (2) French mutation primer: 5′-cagatgacctgacaacccCgatcatcatggacgtacagaaac-3′, 80877-80918. (3) Belgian mutation primer: 5′-agaacaggggaggttccacaAtgaaaacacagatgacctgac-3′, 80848-80889. The sequence and correct integration were verified by sequencing. Titin exons are based on the complete titin gene, *TTN* (*Homo sapiens* titin; GeneID: 7273, HGNC:12403).

GST pulldown assay

GST pulldown assays were essentially performed as described (Lange et al., 2002). Cos1 cells transfected with pEGFP-fusion constructs were extracted with IP buffer [10 mM Tris-HCl (pH 7.9), 150 mM NaCl, 0.5% NP-40, 1 mM DTT supplemented with a protease inhibitor cocktail (Roche)] and the cell lysates were incubated with certain amounts of beads coupled with GST fusion proteins for 2 hours on ice. Following incubation, beads were washed four times in IP buffer. The proteins retained on the beads were separated on SDS-PAGE and then transferred onto nitrocellulose membrane following standard procedures. Blots were treated with mouse monoclonal anti-GFP (Roche) and subsequently with a secondary antibody [HRP-conjugated anti-mouse (DAKO Cytomation, Glostrup, Denmark)]. Detection was performed by ECL western blotting analysis system following the manufacturer's manual [Amersham (GE Healthcare)].

Cell culture and transfection

NRCs were isolated from rats and cultured essentially as described (Lange et al., 2002). NRC was transfected with pEGFP-fusion constructs using Escort III (Sigma-Aldrich) following the manufacturer's manual. After changing medium to NRC maintenance medium (78% DMEM, 19.4% Medium M199, 4% horse serum, 1% penicillin/streptomycin, 4 mM glutamine, 0.1 mM phenylephrine), cells were cultured for another 48 hours to promote the expression.

Immunostaining

Cryosections were fixed with pre-chilled acetone for 5 minutes at –20°C. NRCs were fixed with 4% paraformaldehyde in PBS for 6 minutes, then neutralized with 0.1 M Glycine in PBS and permeabilized with 0.2% Triton X-100 in PBS. After washing with PBS, the sample was blocked with 5% normal goat serum/1% BSA in GB [20 mM Tris-HCl (pH 7.5), 155 mM NaCl, 2 mM EGTA, 2 mM $MgCl_2$] for 30 minutes. The sample was incubated with primary antibody in 1% BSA/GB for 1 hour and, after washing with PBS, was incubated with secondary antibody in 1% BSA/GB for 1 hour. Following sufficient washing with PBS, the sample was mounted in mounting medium [30 mM Tris-HCl (pH 9.5), 70% Glycerol, 5% n-propyl gallate]. All processes were performed at room temperature except for acetone fixation.

Antibodies

Three antibodies used as primary antibodies for immunostaining are described below. T51: mouse monoclonal antibody raised against titin M9 Ig domain (Obermann et al., 1996); Myomesin B4: mouse monoclonal antibody raised against myomesin domain My12 (Grove et al., 1984); Ob58-59 [former Ob48-49, re-named after genomic analysis (Fukuzawa et al., 2005)]: rabbit polyclonal antibody raised against two Ig domains; Ob58 (exOb48) and Ob59 (exOb49) (Young et al., 2001). A rabbit polyclonal antibody was raised against recombinant Obsl1-Ig1 and affinity purified against the antigen as described (Harlow and Lane, 1988). All fluorescent-conjugated secondary antibodies were purchased from Jackson ImmunoResearch (USA).

Confocal microscopy and image analysis

Cell preparations and tissue sections were imaged with a Zeiss LSM510 confocal microscope in sequential scanning mode, using a 63× oil-immersion objective and instrument zoom rates between 1× and 2.5×.

Ratiometry

To see whether GFP-X expression affected blue protein expression, images were imported into Mathematica 5.2 for ratiometric analysis. Briefly, each channel of a 24-bit RGB image was filtered with a 3×3 boxed mean filter to dampen noise. The blue channel was then normalized by division with the red channel. Noise-dependent division artefacts were suppressed by converting very low intensity red pixels (<10% of dynamic range) into large values (100× dynamic range). The green channel containing the GFP signal was then extracted and thresholded to obtain a mask that covered the whole GFP-X-expressing cell(s). This enabled automatic extraction of two subsets of pixels from the red-normalized blue channel, those coincident with the GFP mask, and the rest lying outside of this mask. A histogram of normalized values for each subset was then created from which the weighted mean normalized intensity values were calculated for the GFP-positive subset and the GFP-negative subset. The ratio of these two values (GFP-positive:GFP-negative) was then calculated. This value indicated whether expression of GFP-fusion proteins increased or decreased blue protein levels (increased and decreased ratio respectively).

This work was supported by the Volkswagen Foundation and the Medical Research Council of Great Britain (A.F. and M.G.), and the EU network of excellence MYORES (A.F., S.L. and M.G.). We are gratefully indebted to Pamela Taylor-Harris and Elisabeth Ehler for cardiomyocyte preparations.

References

Agarkova, I. and Perriard, J. C. (2005). The M-band: an elastic web that crosslinks thick filaments in the center of the sarcomere. *Trends Cell Biol.* **15**, 477-485.

Agarkova, I., Ehler, E., Lange, S., Schoenauer, R. and Perriard, J. C. (2003). M-band: a safeguard for sarcomere stability? *J. Muscle Res. Cell Motil.* **24**, 191-203.

Agarkova, I., Schoenauer, R., Ehler, E., Carlsson, L., Carlsson, E., Thornell, L. E. and Perriard, J. C. (2004). The molecular composition of the sarcomeric M-band correlates with muscle fiber type. *Eur. J. Cell Biol.* **83**, 193-204.

Agarkova, I., Schoenauer, R., Perriard, J. C. and Lange, S. (2006). Addition to myomesin's family: expression and properties of novel sarcomeric M-band component, myom3. *J. Muscle Res. Cell Motil.* **27**, 507.

Armani, A., Galli, S., Giacomello, E., Bagnato, P., Barone, V., Rossi, D. and Sorrentino, V. (2006). Molecular interactions with obscurin are involved in the localization of muscle-

specific small ankyrin1 isoforms to subcompartments of the sarcoplasmic reticulum. *Exp. Cell Res*. **312**, 3546-3558.

Bagnato, P., Barone, V., Giacomello, E., Rossi, D. and Sorrentino, V. (2003). Binding of an ankyrin-1 isoform to obscurin suggests a molecular link between the sarcoplasmic reticulum and myofibrils in striated muscles. *J. Cell Biol.* **160**, 245-253.

Borisov, A. B., Raeker, M. O., Kontrogianni-Konstantopoulos, A., Yang, K., Kurnit, D. M., Bloch, R. J. and Russell, M. W. (2003). Rapid response of cardiac obscurin gene cluster to aortic stenosis: differential activation of Rho-GEF and MLCK and involvement in hypertrophic growth. *Biochem. Biophys. Res. Commun.* **310**, 910-918.

Brummelkamp, T. R., Bernards, R. and Agami, R. (2002). A system for stable expression of short interfering RNAs in mammalian cells. *Science* **296**, 550-553.

Carmignac, V., Salih, M. A. M., Quijano-Roy, S., Marchand, S., Al Rayess, M. M., Mukhtar, M. M., Urtizberea, J. A., Labeit, S., Guicheney, P., Leturcq, F. et al. (2007). C-terminal titin deletions cause a novel early-onset myopathy with fatal cardiomyopathy. *Ann. Neurol.* **61**, 340-351.

Ferrara, T. M., Flaherty, D. B. and Benian, G. M. (2005). Titin/connectin-related proteins in C. elegans: a review and new findings. *J. Muscle Res. Cell Motil.* **26**, 435-447.

Fukuzawa, A., Idowu, S. and Gautel, M. (2005). Complete human gene structure of obscurin: implications for isoform generation by differential splicing. *J. Muscle Res. Cell Motil.* **26**, 427-434.

Geisler, S. B., Robinson, D., Hauringa, M., Raeker, M. O., Borisov, A. B., Westfall, M. V. and Russell, M. W. (2007). Obscurin-like 1, OBSL1, is a novel cytoskeletal protein related to obscurin. *Genomics* **4**, 521-531.

Gotthardt, M., Hammer, R. E., Hubner, N., Monti, J., Witt, C. C., McNabb, M., Richardson, J. A., Granzier, H., Labeit, S. and Herz, J. (2002). Conditional expression of mutant M-line titins results in cardiomyopathy with altered sarcomere structure. *J. Biol. Chem.* **278**, 6059-6065.

Grove, B. K., Kurer, V., Lehner, C., Doetschman, T. C., Perriard, J. C. and Eppenberger, H. M. (1984). A new 185,000-dalton skeletal muscle protein detected by monoclonal antibodies. *J. Cell Biol.* **98**, 518-524.

Hackman, P., Vihola, A., Haravuori, H., Marchand, S., Sarparanta, J., De Seze, J., Labeit, S., Witt, C., Peltonen, L., Richard, I. et al. (2002). Tibial muscular dystrophy is a titinopathy caused by mutations in TTN, the gene encoding the giant skeletal-muscle protein titin. *Am. J. Hum. Genet.* **71**, 492-500.

Harlow, E. and Lane, D. (1988). *Antibodies, A Laboratory Manual*. Cold Spring Harbor, NY: Cold Spring Harbor Laboratory Press.

Hoshijima, M. (2006). Mechanical stress-strain sensors embedded in cardiac cytoskeleton: Z disk, titin, and associated structures. *Am. J. Physiol. Heart Circ. Physiol.* **290**, H1313-H1325.

Kontrogianni-Konstantopoulos, A., Jones, E. M., Van Rossum, D. B. and Bloch, R. J. (2003). Obscurin is a ligand for small ankyrin 1 in skeletal muscle. *Mol. Biol. Cell* **14**, 1138-1148.

Kontrogianni-Konstantopoulos, A., Catino, D. H., Strong, J. C., Sutter, S., Borisov, A. B., Pumplin, D. W., Russell, M. W. and Bloch, R. J. (2006). Obscurin modulates the assembly and organization of sarcomeres and the sarcoplasmic reticulum. *FASEB J.* **20**, 2102-2111.

Lange, S., Auerbach, D., McLoughlin, P., Perriard, E., Schafer, B. W., Perriard, J. C. and Ehler, E. (2002). Subcellular targeting of metabolic enzymes to titin in heart muscle may be mediated by DRAL/FHL-2. *J. Cell Sci.* **115**, 4925-4936.

Lange, S., Ehler, E. and Gautel, M. (2006). From A to Z and back? Multicompartment proteins in the sarcomere. *Trends Cell Biol.* **16**, 11-18.

Linke, W. A. (2008). Sense and stretchability: the role of titin and titin-associated proteins in myocardial stress-sensing and mechanical dysfunction. *Cardiovasc. Res.* **77**, 637-648.

Musa, H., Meek, S., Gautel, M., Peddie, D., Smith, A. J. H. and Peckham, M. (2006). Targeted homozygous deletion of M-band titin in cardiomyocytes prevents sarcomere formation. *J. Cell Sci.* **119**, 4322-4331.

Obermann, W. M. J., Gautel, M., Steiner, F., Van der Ven, P., Weber, K. and Fürst, D. O. (1996). The structure of the sarcomeric M band: localization of defined domains of myomesin, M-protein and the 250 kD carboxy-terminal region of titin by immunoelectron microscopy. *J. Cell Biol.* **134**, 1441-1453.

Obermann, W. M. J., Gautel, M., Weber, K. and Fürst, D. O. (1997). Molecular structure of the sarcomeric M band: mapping of titin- and myosin-binding domains in myomesin and the identification of a potential regulatory phosphorylation site in myomesin. *EMBO J.* **16**, 211-220.

Peng, J., Raddatz, K., Labeit, S., Granzier, H. and Gotthardt, M. (2006). Muscle atrophy in titin M-line deficient mice. *J. Muscle Res. Cell Motil.* **26**, 381-388.

Peng, J., Raddatz, K., Molkentin, J. D., Wu, Y., Labeit, S., Granzier, H. and Gotthardt, M. (2007). Cardiac hypertrophy and reduced contractility in hearts deficient in the titin kinase region. *Circulation* **115**, 743-751.

Raeker, M. O., Su, F., Geisler, S. B., Borisov, A. B., Kontrogianni-Konstantopoulos, A., Lyons, S. E. and Russell, M. W. (2006). Obscurin is required for the lateral alignment of striated myofibrils in zebrafish. *Dev. Dyn.* **235**, 2018-2029.

Russell, M. W., Raeker, M. O., Korytkowski, K. A. and Sonneman, K. J. (2002). Identification, tissue expression and chromosomal localization of human Obscurin-MLCK, a member of the titin and Dbl families of myosin light chain kinases. *Gene* **282**, 237-246.

Salih, M. A., Al Rayess, M., Cutshall, S., Urtizberea, J. A., Al-Turaiki, M. H., Ozo, C. O., Straub, V., Akbar, M., Abid, M., Andeejani, A. et al. (1998). A novel form of familial congenital muscular dystrophy in two adolescents. *Neuropediatrics* **29**, 289-293.

Schoenauer, R., Lange, S., Hirschy, A., Ehler, E., Perriard, J. C. and Agarkova, I. (2008). Myomesin 3, a novel structural component of the M-band in striated muscle. *J. Mol. Biol.* **376**, 338-351.

Subahi, S. A. (2001). Distinguishing cardiac features of a novel form of congenital muscular dystrophy (Salih cmd). *Pediatr. Cardiol.* **22**, 297-301.

Tskhovrebova, L. and Trinick, J. (2003). Titin: properties and family relationships. *Nat. Rev. Mol. Cell Biol.* **4**, 679-689.

Udd, B., Vihola, A., Sarparanta, J., Richard, I. and Hackman, P. (2005). Titinopathies and extension of the M-line mutation phenotype beyond distal myopathy and LGMD2J. *Neurology* **64**, 636-642.

Van den Bergh, P. Y., Bouquiaux, O., Verellen, C., Marchand, S., Richard, I., Hackman, P. and Udd, B. (2003). Tibial muscular dystrophy in a Belgian family. *Ann. Neurol.* **54**, 248-251.

Young, P., Ferguson, C., Banuelos, S. and Gautel, M. (1998). Molecular structure of the sarcomeric Z-disk: two types of titin interactions lead to an asymmetrical sorting of alpha-actinin. *EMBO J.* **17**, 1614-1624.

Young, P., Ehler, E. and Gautel, M. (2001). Obscurin, a giant sarcomeric Rho guanine nucleotide exchange factor protein involved in sarcomere assembly. *J. Cell Biol.* **154**, 123-136.

Journal of Cell Science

Supplemental Figure 1

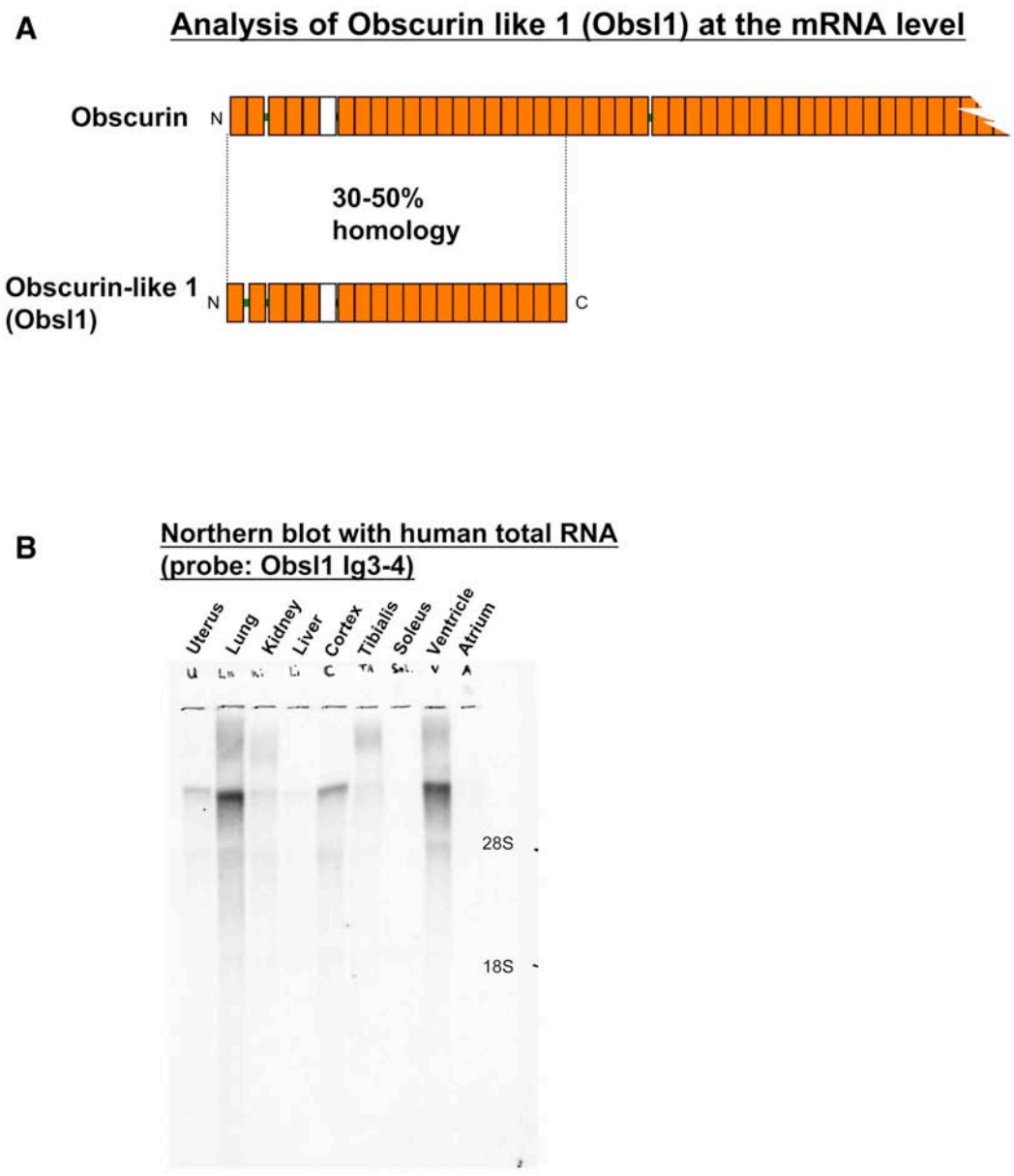

(A) Obsl1 has sequence homology to the N-terminal 20 domains of obscurin and shares the domain pattern of tandem Ig domains and one fibronectin C3 domain. (B) The protein is widely expressed, as detected by Northern blots, but preferentially in striated muscles. However, also tissues with significant smooth muscle components such as lung and uterus express Obsl1. As with obscurin, multiple splice variants may be expressed.

Supplemental Figure 2 A,B,C

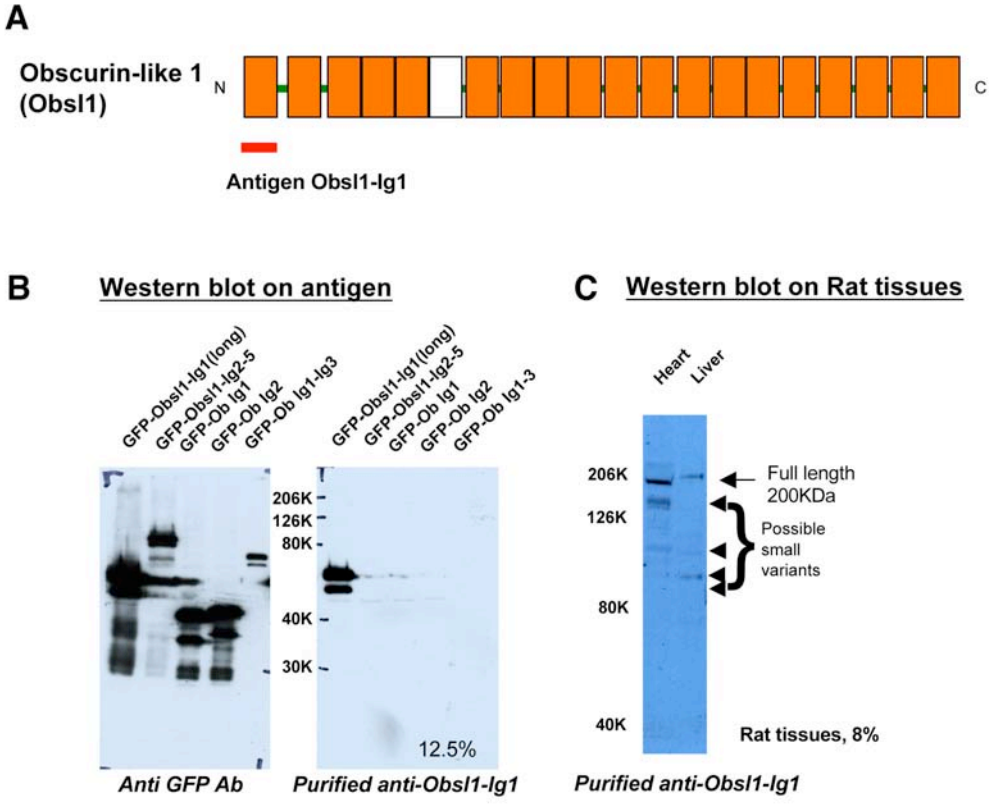

(**A**) rabbit polyclonal antibody was raised against Obsl1 Ig domain 1 and affinity purified on the antigen. (**B**) Western blots of COS1 cells transfected with various GFP-tagged Obsl1 and obscurin constructs demonstrates that this antibody specifically recognised Obsl1. (**C**) Western blots in rat tissues detect a dominant ca. 200 kDa band in heart ventricles; fainter bands are also detected in liver and other tissues. Smaller and fainter bands detected may be splice variants.

Supplemental Figure 2 C and D

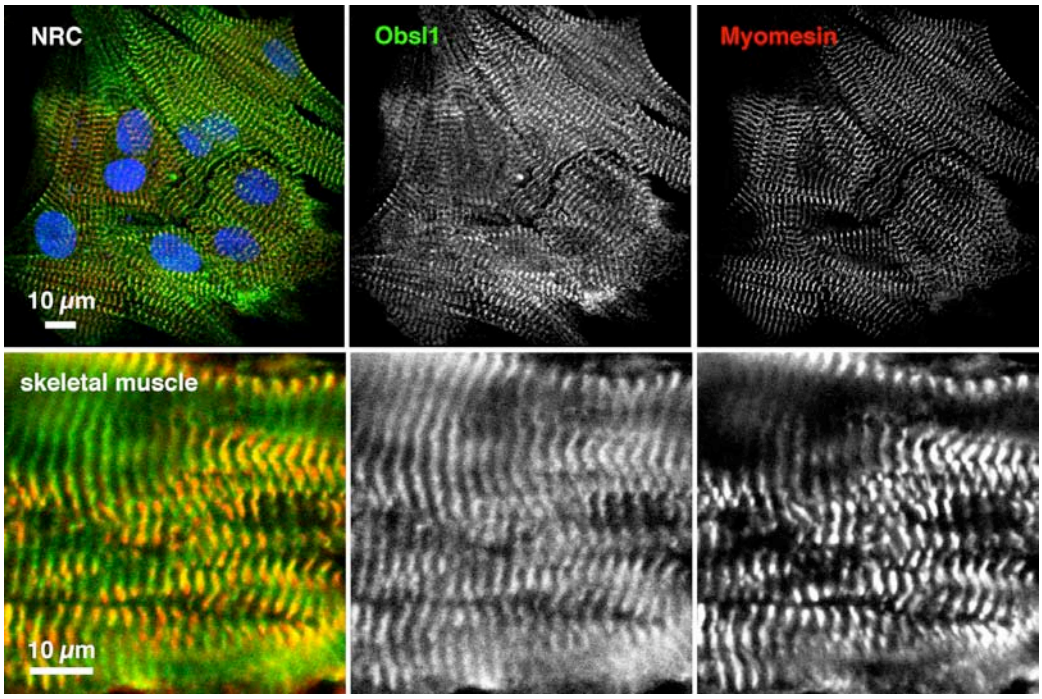

(**C**) The Obsl1-Ig1 antibody stains M-bands in neonatal rat cardiomyocytes (NRC) as well as in longitudinal sections of skeletal muscle, as visualized by counterstain with anti-Myomesin antibodies. Intercalated disks in NRC are not stained by anti-obsl1-Ig1. Nuclei in the NRC overlay in blue.

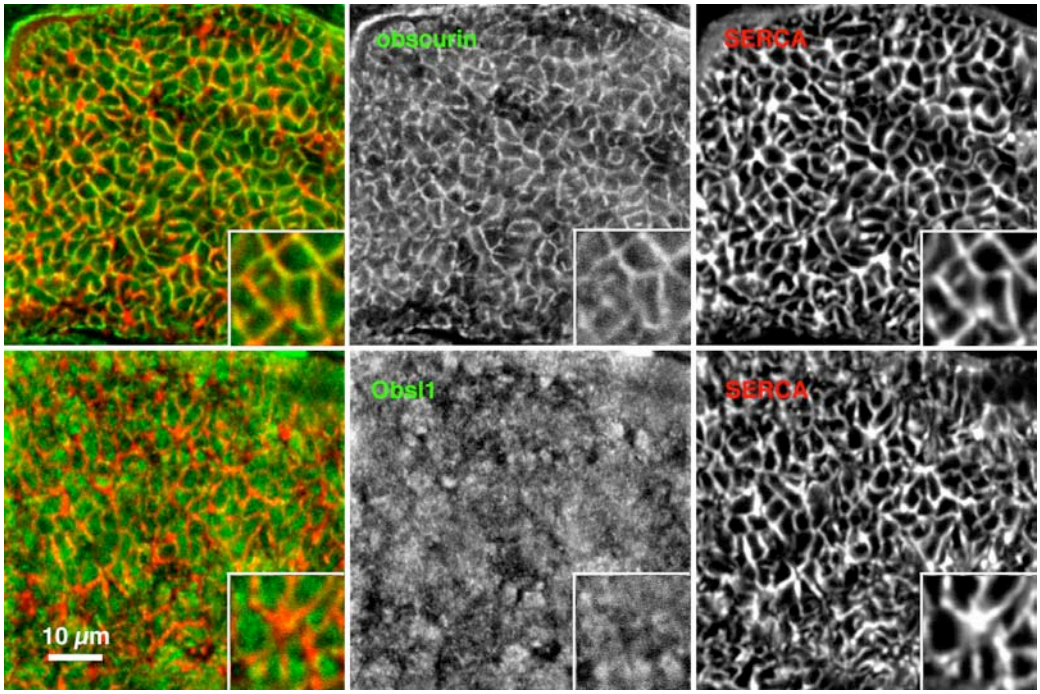

(**D**) In transverse sections of skeletal muscle (here: slow fibres), obscurin stains a perimyofibrillar pattern coinciding with SERCA. The obsl1-Ig1 antibody staining reveals a predominantly myofibrillar pattern surrounded by SERCA-positive sarcoplasmic reticulum. Inserts: 2-fold magnifications.